Experimental Demonstration of Spatial Hole Burning Reduction Leading to 1480-nm Pump Lasers Output Power Improvement

Ali Guermache, Vincent Voiriot, Damien Locatelli, Frédéric Legrand, Rose-Marie Capella, Philippe Gallion, and Joël Jacquet

***Abstract*—Observation of spatial hole burning reduction is reported for the first time to our knowledge on flared 1480-nm high-power InGaAsP–InP buried ridge lasers. We determined the longitudinal carrier density profile by spatially resolved spontaneous emission measurements for slightly tapered and straight active waveguides. The tapered stripe shows spatial hole burning reduction leading to 25% output power enhancement.**

***Index Terms*—Flared waveguide, pump lasers, semiconductor lasers.**

I. Introduction

RECENT progress in data transmission systems requires high output power single transverse mode laser diodes for Raman and erbium-doped fiber amplifier pump sources. Several approaches have shown high output power emission [1]–[3]; the design rules in these papers are mainly related to the active volume increase through large [1] or flared [2] waveguides or the use of multimode interferometer [3]. Such designs lead to electrical and thermal resistance decrease and slope efficiency of the light–current (L–I) characteristic increase. Flared waveguides have been initially proposed for 980-nm pump lasers in order to reduce photon density close to the antireflection coating facet and, as a consequence, limit the catastrophic optical mirror damage at high output power [4]. In this work, we compare the longitudinal carrier density distribution in straight and flared buried ridge InGaAsP–InP pump lasers using the spontaneous emission measurement method [5]–[7]. In such lasers, high and low reflectivity mirrors are deposited at the rear and front facets, respectively. The asymmetric reflectivities are at the origin of inhomogeneous photon distribution along the cavity that induces inhomogeneous carrier distribution through stimulated emission process. Measurements show a much flatter carrier profile along the cavity associated with a higher maximum output power for the flared devices. Flatter longitudinal photon and carrier distributions improve the overall gain of the cavity and reduce the gain saturation at high bias currents. As we are aware, this is the first time that a reduction of longitudinal spatial hole burning (LSHB) in flared devices leading to output power increase is demonstrated experimentally.

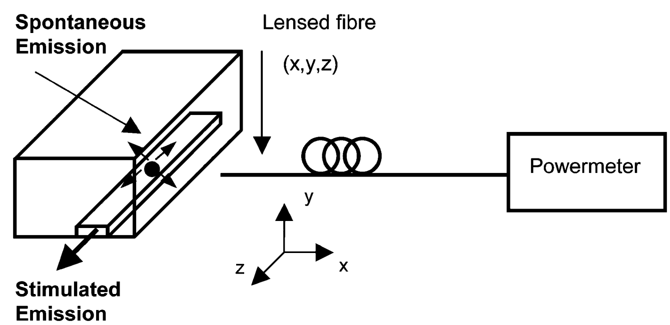

Fig. 1. Experimental setup.

II. Device Structures

The structure is an InGaAsP–InP buried ridge waveguide. The gas source molecular beam epitaxy grown active layer consist of five compressively InGaAsP strained quantum wells separated by four lattice matched barriers. The active layer is sandwiched between two nonintentionally doped 1.17-μm InGaAsP separate confinement layers. The photoluminescence peak is centered at 1470 nm. Selective growth is then performed to realize p-n InP blocking layers on both sides of the dry etched mesa. The ridge is then buried with optimized p-doping profile InP cladding and InGaAs p++ contact layers. Then, metallic contact layers are deposited on both the p- and n-sides.

III. Experimental Setup

The experimental setup is shown in Fig. 1. The collected spontaneous emission rate $(R_{\rm sp})$ [7] is related to the square of the carrier density (N) in the active region by

$$R_{\rm sp} = \alpha(z) \cdot B \cdot N^2(z) \tag{1}$$

where $\alpha(z)$ is the coupling coefficient along z (see Fig. 1), B is the radiative recombination coefficient, and $N(z)$ the carrier density profile along the active stripe. The isotropic character of the spontaneous emitted photons allows collecting spontaneous light from the side of the laser with a lensed fiber. The laser is longitudinally cleaved near the guiding region (50 μm) to optimize the light collection and is mounted onto an AlN submount

Manuscript received November 10, 2004; revised April 15, 2005.

A. Guermache, V. Voiriot, D. Locatelli, F. Legrand, and R.-M. Capella are with Avanex France, Nozay 91625, France (e-mail: ali.guermache@wanadoo.fr; Vincent_Voiriot@avanex.com; Damien_Locatelli@avanex.com; Frederic_Legrand@avanex.com; Rose-Marie_Capella@avanex.com).

P. Gallion is with Ecole Nationale Supérieure des Télécommunications, Paris 75634, France (e-mail: gallion@enst.fr).

J. Jacquet is with Supélec, Metz 57070, France (e-mail: Joel.Jacquet@metz.supelec.fr).

Digital Object Identifier 10.1109/LPT.2005.854386

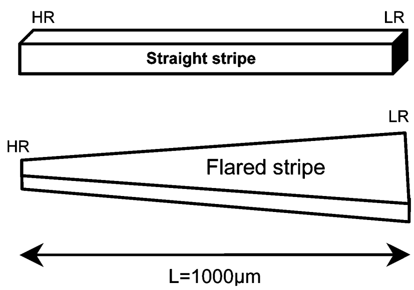

Fig. 2. Straight and flared device schematics.

placed on a copper heatsink. The lensed fiber is mounted on an xyz piezoelectric stage and coupled to an HP 81524A powermeter. Due to the 3-μm spatial resolution of the experimental setup, accurate carrier density profile can be obtained for both flared and straight cavities. The device schematic of such cavities is shown in Fig. 2.

IV. Results and Discussion

Equation (1) shows that carrier density $N(z)$ can be obtained from the spontaneous emission measurements for the different position of the lensed fiber along z and at different current levels for each position. To determine the relative carrier density profile above threshold, a reference measurement is done below threshold for each position. It has been demonstrated in [7] and [8] that the carrier density profile below threshold is constant along the active stripe. Thus, we can obtain the carrier density distribution above threshold normalized to the value below threshold, and the unknown coupling coefficient $\alpha(z)$ in (1) is suppressed.

We have plotted in Fig. 3(a), for a straight waveguide the carriers density profile along the cavity for different currents. Carrier density is maximum on the high reflectivity side and its value increases continuously above threshold when current increases. At the opposite, the carrier density is minimum on the low reflectivity side and decreases for increasing current before increasing again. Such a behavior has already been observed in [8] for broad area lasers and is confirmed here for transverse single mode devices.

Locally the gain can be expressed as follows:

$$g(N,z) = \frac{\Gamma \frac{dg}{dN}[N(z) - N_0]}{1 + \varepsilon S(z)} \tag{2}$$

where $S(z)$ is the photon density, (dg/dN) is the differential gain, Γ the confinement factor and ε is the non linear gain coefficient that generally refers to the spectral hole burning effect.

On the low reflectivity side, the photon density is high and, therefore, the carrier density is low due to stimulated recombination process. In this region, when the current increases, the gain decreases according to (2) on one hand due to the photon density increase and on the other hand through carrier density reduction. To maintain the oscillation condition (i.e., after one round-trip the gain equals the total losses) above threshold, the gain on the high reflectivity side must increase. This is why we observe the increase of carrier density on the rear side of the cavity when current increases [Fig. 3(a)]. Altogether, in such devices, when the current reaches a value around 1 A, the gain saturation close to the output facet becomes the dominant process and the output power saturates.

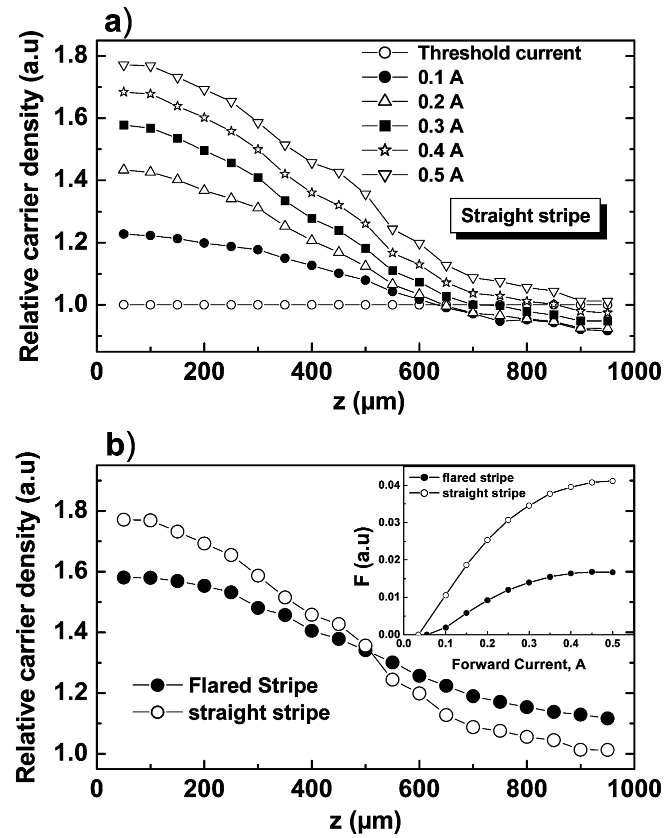

Fig. 3. (a) Longitudinal relative carrier density profile for straight stripe. (b) Longitudinal relative carrier density profile for a straight and a flared stripe at $I = (I_s, I_f)$. Inset: Variance F as a function of current intensity.

In order to limit this effect and to push the power saturation at higher currents, we designed flared devices where the active waveguides widens close to the front facet. This leads, for given output power, to a lower photon density on the low reflectivity side, and to power saturation reduction, as compared to straight waveguides. We expect therefore higher output power with such design.

Lasers including flared and straight active stripes have been fabricated on the same wafer and their characteristics are compared in the following. The cavity length is 1000 μm and both flared and straight chip facets were coated simultaneously. The reflectivities of the rear $(z = 0)$ and front $(z = 1000)$ facets are 95% and 0.1%, respectively. The widths of the straight and flared stripes at the rear facet are about 3 μm, and at the front facet, the width of the flared stripe is less than 10 μm in order to maintain single transverse mode operation at high power. All measurements were done at room temperature, $T = 25\ ^\circ$C.

As the LSHB effect is maximum for high power level, we compare in Fig. 3(b) the longitudinal carrier density distribution for straight and flared waveguides at their respective saturation currents I_s and I_f. The saturation currents are defined as the currents corresponding to maximum output power. As expected, the carrier density is found more uniform in the case of flared

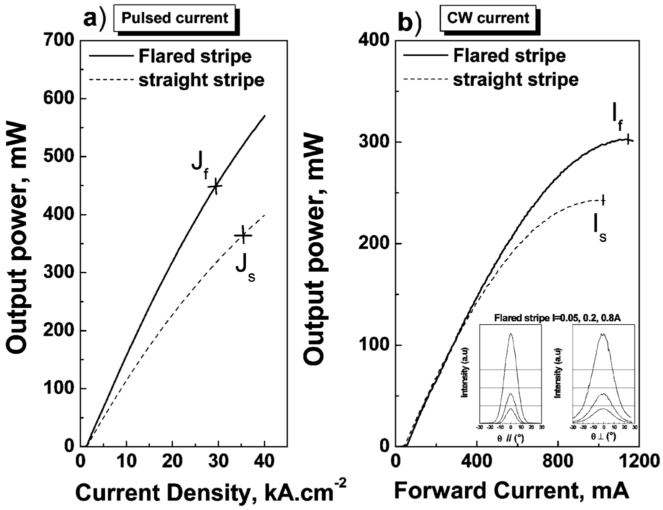

Fig. 4. (a) Output power as a function of current density under pulsed operation (pulse width $= 300$ ns at 10 kHz). (b) Output power as a function of current intensity under CW operation. Inset: Far-field pattern for the flared stripe. J_s current density corresponding to I_s, I_s saturation current for the straight laser J_f current density corresponding to I_f, I_f saturation current for the flared laser.

laser. We introduce the variance parameter F (3), to quantify the carrier profile flatness (i.e., the spatial hole burning) as in [9]

$$F = \frac{1}{L}\int_0^L \left(\frac{N(z)-\overline{N}}{\overline{N}}\right)^2 dz \tag{3}$$

where L is the cavity length and $\overline{N}$ the average carrier density value.

In the inset of Fig. 3(b), the F factor is plotted as function of the current for both straight and flared devices. As expected, F is lower for the flared waveguides, as compared to straight one. A reduction of the variance by a factor larger than two, from 4×10^{-2} (straight) to 1.6×10^{-2} (flared) is deduced at 0.5 A from the inset of Fig. 3(b). An improvement of the output power figure is, therefore, expected with this flared laser.

It is confirmed in Fig. 4(a), where the power–current characteristic shows a clear improvement in the case of the flared structure as compared to the straight one. This improvement occurs as soon as the threshold is reached. Experiment depicted in Fig. 4(a) is done under pulsed current injection (pulsewidth: 300 ns at 10 kHz) to be free from thermal effect that can strongly affect power saturation in continuous-wave (CW) regime. In addition, we plot the power characteristic as a function of the current density to take into account the difference of the active volume between both structures. As a consequence, we can conclude that LSHB reduction observed in Fig. 3(b) is the only factor that leads to power increase in flared structure. However, this point is to be confirmed in CW regime.

This is done in Fig. 4(b) where the L–I characteristic is plotted for both waveguide types. The maximum output power is 25% higher for the flared device at the saturation currents (305 versus 245 mW at I_f and I_s). It is important to note that saturation currents defined in Fig. 4(b), I_f and I_s, when reported in current density J_s and J_f in Fig. 4(a), leads to the same power increase of around 25% [from 360 mW at J_s to 445 mW at J_f, see Fig. 4(a)]. This confirms the consistency of our results and the strong impact of the LSHB on power saturation in pump lasers. Moreover, the flared stripe shows a single transverse mode operation in CW regime for I varying from 0.05 A to 0.8 A [see inset Fig. 4(b)].

V. Conclusion

We experimentally demonstrate that nonuniform carrier and photon distributions along pump laser are one of the main origins of power saturation for asymmetric cavity pump lasers. Using spatially resolved spontaneous emission measurement, we demonstrate that for slightly flared active waveguide, better carrier uniformity is recorded. A 25% maximum output power improvement is obtained with this flared device as compared to straight waveguide from the same wafer, which is attributed to the longitudinal spatial hole burning reduction.

References

[1] D. Garbuzov, A. Komissar, I. Kudryashov, M. Maiorov, R. Roff, and J. Connolly, "High power Raman pumps based on ridge waveguide in InGaAsP/InP diode lasers," in *Optical Fiber Communication Conf.*, 2003, pp. 394–396.

[2] S. Delepine, F. Gerard, A. Pinquier, T. Fillion, J. Pasquier, D. Locatelli, J.-P. Chardon, H. K. Bissessur, N. Bouche, F. R. Boubal, and P. Salet, "How to launch 1 W into single-mode fiber from a single 1.48-μm flared resonator," *IEEE J. Sel. Topics Quantum Electron.*, vol. 7, no. 2, pp. 111–123, Mar./Apr. 2001.

[3] K. Hamamoto, K. Naniwae, and M. Ohya, "High power with low electric power consumption active multi-mode interferometer laser diode for fiber amplifier," *Electron. Lett.*, vol. 38, pp. 517–519, 2002.

[4] M. Sagawa, K. Hiramoto, T. Toyonaka, T. Kikawa, S. Fujisaki, and K. Uomi, "Highly reliable and stable lateral mode operation of high power 0.98 μm InGaAs-InGaAsP lasers with an exponential shaped flared stripe," *IEEE J. Sel. Topics Quantum Electron.*, vol. 3, no. 2, pp. 666–671, Apr. 1997.

[5] P. Blood, A. I. Kucharska, C. T. Foxon, and K. Griffiths, "Temperature dependence of spontaneous emission in GaAs-AlGaAs quantum well lasers," *Appl. Phys. Lett.*, vol. 55, pp. 1167–1169, 1989.

[6] G. M. Lewis, P. M. Smowton, J. D. Thomson, H. D. Summers, and P. Blood, "Measurement of true spontaneous emission spectra from the facet of diode laser structures," *Appl. Phys. Lett.*, vol. 80, pp. 1–3, 2002.

[7] F. Girardin, G. H. Duan, C. Chabran, P. Gallion, M. Blez, and M. Allovan, "Determination of nonlinear gain coefficient of semiconductor lasers from above threshold spontaneous emission measurement," *IEEE Photon. Technol. Lett.*, vol. 6, no. 8, pp. 894–896, Aug. 1994.

[8] F. Rinner, J. Rogg, P. Friedmann, M. Mikulla, R. Propawe, and G. Weimann, "Longitudinal carrier density measurement of high power broad area laser diodes," *Appl. Phys. Lett.*, vol. 80, pp. 19–21, 2002.

[9] H. Soda, Y. Kotaki, H. Sudo, H. Ishikawa, S. Yamakoshi, and H. Imai, "Stability in single longitudinal mode operation in GaInAsP/InP phase-adjusted DFB lasers," *IEEE J. Quantum Electron.*, vol. 23, no. 6, pp. 804–814, Jun. 1987.